

# Electrochemical Performance of Carbon derived from Bamboo Shoot as Anode Materials for Lithium-ion Battery

Zhengping Zhao<sup>1,2</sup>, Sitao Shen<sup>2</sup>, Yuting Li<sup>2</sup>, Qiaodian Chen<sup>1</sup>, Mingqiang Zhong<sup>2</sup> and Xiufang Chen<sup>3,\*</sup>

<sup>1</sup> Zhijiang College, Zhejiang University of Technology, Hangzhou, 310014, China

<sup>2</sup> College of Materials Science and Engineering, Zhejiang University of Technology, Hangzhou 310014, China

<sup>3</sup> College of Materials Science and Engineering, Zhejiang University of Science and Technology, Hangzhou 310018, China

\*E-mail: [chenxf@zstu.edu.cn](mailto:chenxf@zstu.edu.cn)

Received: 5 January 2020 / Accepted: 10 February 2020 / Published: 10 April 2020

---

Renewable bamboo shoot is carbonized and used as anode material for lithium ion battery to study its electrochemical properties. The average pore diameter of the carbon micropores of the bamboo shoot powder is 19-20 nm, the specific area is as high as 1126.18 m<sup>2</sup>/g and can be controlled by the carbonization temperature. When the current density is 1.0 Ag<sup>-1</sup>, the unit capacitance is 575 mAh/g and the specific capacity retention rate is 78.2% after charging and discharging 50 times. After processing, bamboo shoot carbon has the equivalent specific capacity of petroleum carbon materials for market sale, which provides a new idea for the development and utilization of bamboo industry.

---

**Keywords:** Bamboo shoot, Carbonization, Anode Materials, Electrochemical properties

## 1. INTRODUCTION

Lithium-ion batteries, the most important electrical energy storage device, have been widely used in a variety of portable devices, energy storage devices and hybrid vehicles, which are vital to alleviate the energy crisis and global environmental problems [1-3]. Lithium-ion battery is one of the most important chemical energy sources in secondary batteries, which has attracted great attention in the past decades. Demand for lithium-ion batteries is growing rapidly, especially for electric vehicles, which are expected to require nearly 100 kilowatts per hour to meet consumer demand for electric vehicles. It will also be used to buffer intermittent supply from renewable and volatile green sources and to balance differences between energy supply and demand. [4].

Nowadays, most of anode materials for lithium ion batteries are carbon materials, such as carbon fiber, natural graphite and artificial modified graphite. In recent years, the research on the anode

materials of lithium ion batteries are mainly focuses on the surface modification of carbon materials, the adhesion of nano phases , the formation of nano pores on surface and other applications of nanotechnology [5-8]. Many achievements have been made in this field, which shows that lithium ion batteries have a promising future.

As a kind of renewable resource, bamboo shoot has a wide range of sources and alternative values. Bamboo shoot contains a variety of active functional groups, such as cellulose, lignin, bamboo leaves flavonoids, polysaccharides, amino acids terpene, alkaloids, phenolic acids, volatile components, etc. [9-10]. Bamboo shoot carbon is a kind of porous carbon which is formed from bamboo shoot powder by hydrothermal reaction and high-temperature carbonization. The raw materials are abundant, cheap, with the characteristics of high specific surface area, excellent chemical stability, adjustable pore size and uniform pore size distribution. A large amount of carbon materials can be obtained after carbonization, which has potential application value.

Natural bamboo shoot carbon is carbonized and used as anode material of lithium ion battery to study its electrochemical properties. The electrochemical properties were tested and analyzed to develop a kind of high performance lithium-ion battery anode material which can utilize bamboo as carbon source.

## 2. EXPERIMENTAL SECTION

### 2.1 Materials

Bamboo shoot, isopropyl alcohol, sodium molybdate, thiourea, potassium hydroxide, acetylene black, N-methylpyrrolidone and polyvinylidene fluoride (PVDF) were all analytical reagents purchased from Shanghai Chemical Reagents Corp (Shanghai, China).

### 2.2 Preparation of bamboo shoot carbon

2 g bamboo shoot powder and 8 g potassium bicarbonate ( $\text{KHCO}_3$ ) were dissolved in 15 mL deionized water. Ultrasonic 10 min, stirring 2 h at room temperature, heating to 180 °C constant temperature 5.5 h, cooling grinding mix evenly. Heat in  $\text{N}_2$  (100 mL/min) to 600 °C (10 °C /min), keep warm for 1 h, reduce to room temperature and grind to powder. Bamboo shoot carbon (PC-1) was obtained by washing with 5% HCl solution and drying in vacuum (80 °C).

2 g bamboo shoot powder and 8 g potassium bicarbonate ( $\text{KHCO}_3$ ) were dissolved in 15 mL deionized water. Ultrasonic 10 min, stirring 2 h at room temperature, heating to 180 °C constant temperature 5.5 h, cooling grinding mix evenly. Heat in  $\text{N}_2$  (100 mL/min) to 900 °C (10 °C /min), keep warm for 1 h, reduce to room temperature and grind to powder. Bamboo shoot carbon (PC-2) was obtained by washing with 5% HCl solution and drying in vacuum (80 °C). The preparation process is shown in figure 1.

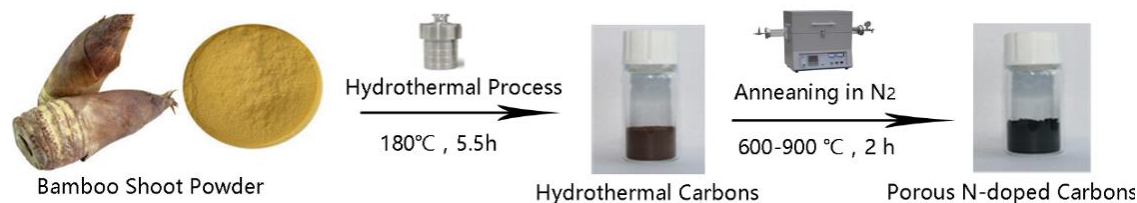


**Figure 1.** Preparation process of bamboo shoot carbon

### 2.3 Battery assembly

Copper sheets with a radius of 1 cm were prepared by tablet pressing mechanism. Ethanol ultrasonic cleaning, blow-drying and weighing of each copper sheet were conducted. Acetylene black is grinding sieving reserve. PVDF and NMP were configured as conductive gels at a mass ratio of 1:10. Dissolved under 55 °C, and stirring until the gel without air bubbles once every 15 min. PC, acetylene black and conductive gel were added to the sample bottle at a ratio of 8:1:1. An appropriate amount of NMP was added, stirred for 30 min and the sample was coated on the copper sheet. Dry electrodes with pressing machine, then vacuum drying at 60 °C by for 24 hours to prepare electrode materials and assembled into CR 2025 button cell [11].

### 2.4 Characterization

FT-IR spectra of all samples were recorded using polymer granule on a Perkin-Elmer Wellesley MA spectrophotometer. Thermogravimetric analysis (TGA) was performed on a TGA 7 instrument (PerkinElmer) thermal analysis system. Sample weight taken was 2-4 mg. All the experiment data were taken as an average of at least five measurements. The microstructures were observed on a Scanning Electron Microscope (Hitachi S4000, Japanese) and a Transmission Electron Microscope (JEM-100CX II, Japanese). Raman spectroscopy is a method for qualitative analysis of molecular structure. The chemical structures were observed on a Lab RAM HR UV800 laser Raman spectrometer (JOBIN YVON, France). The excitation light source is 632.81 nm and the scanning range is 200~4000. The XPS (KRATOS AXIS Ultra DLD, Shimadzu KRATOS) was used. The light source was Al-KαX rays and the vacuum degree was  $3 \times 10^{-7}$  Pa. Nitrogen adsorption test (BET) was using the automatic physical adsorption instrument (ASAP2020, mack instruments). X-ray diffractometer (X'pert PRO, PANalytical) was used. The test parameters of the instrument are as follows: 36 kV, 30 mA and Cu radiation.

The constant charge-discharge performance was tested after the sample electrode material was assembled into CR 2025 button battery. The electrochemical performances such as power density, energy density and specific capacitance can be obtained by processing and analyzing the results of constant current charge-discharge test [14]. The calculation formula of specific capacitance is:

$$Cs = I\Delta t/m\Delta V \quad (1-1)$$

Where  $I(A)$  is the charge-discharge current.  $\Delta t$  for discharge time.  $m$  is the mass of the active substance in the electrode material.  $\Delta V$  is the discharge voltage range.

The cyclic voltammetry is to discuss the reaction of capacitor electrode after applying triangular

waveform potential. The applied control signal is potential, and the measured corresponding signal is current. It is mainly to study the change rules of I-t and I-U. The relation curve of U-I can be obtained by observing the T-t graph [12].

### 3. RESULTS AND DISCUSSION

As is known to all, bamboo shoot has low lignification, less crystalline cellulose, and their chemical composition and physical structure are different from that of mature bamboo. This structure is conducive to the transport of water molecules, and easy to decompose into tiny nanoparticles during the hydrothermal process at the same time. Thus, it can be converted into carbon materials with nanopores.

The morphology and structure of bamboo shoot carbon were characterized by SEM, as shown in figure 2 and figure 3. Obviously, PC-1 shows a loose structure. Carbon particles of bamboo shoot are well dispersed in ethanol solution. For comparison, porous carbon PC-2 was prepared at a higher heat treatment temperature (900 °C). The carbon morphology of the two kinds of bamboo shoot was basically similar, indicating that sintering temperature had little effect on the macroscopic morphology of bamboo shoot carbon.

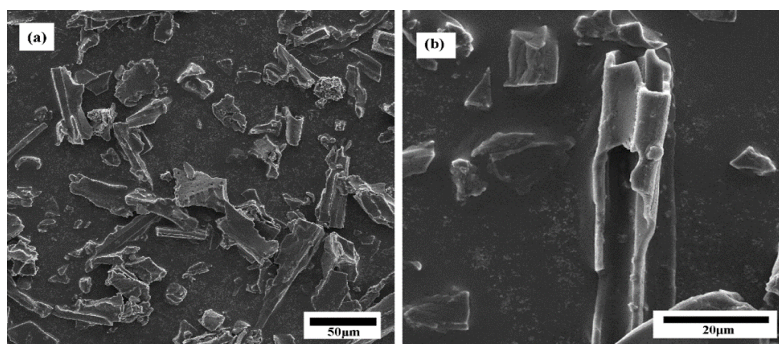


**Figure 2.** SEM images of bamboo shoot carbon (PC-1) at different magnifications, (a) 500X, (b) 2000X

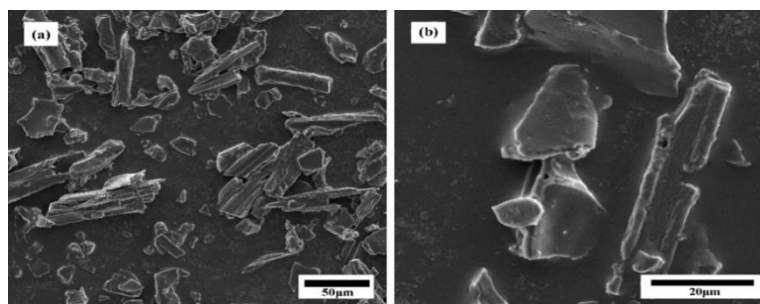


**Figure 3.** SEM images of bamboo shoot carbon (PC-2) at different magnifications, (a) 500X, (b) 2000X

In order to further study the effect of water heat treatment and carbonization temperature on the porous structure of bamboo shoot carbons, N<sub>2</sub> adsorption test was conducted at 77 K temperature. Figure

4 shows the adsorption/desorption curve of bamboo shoot carbon. It can be seen from the adsorption and desorption curve that the two kinds of bamboo shoot carbon have obvious adsorption effect at low pressure ( $<0.1$ , relative pressure  $P/P_0$ ), which indicated that there are a lot of micropores in bamboo shoot carbon particles [13]. In the low pressure area, the adsorption and desorption curves are close to each other, which indicates that the micropores of bamboo shoot carbon are mainly obtained through water heat treatment and carbonization. In addition, nitrogen adsorption exists in the high pressure zone ( $>0.8$ , relative pressure  $P/P_0$ ), indicating that there is a large surface area. Generally speaking, the total adsorption amount of nitrogen is affected by the carbonization temperature. The higher carbonization temperature, the smaller the specific surface area. The specific surface area of PC-1 should be larger than PC-2, which is consistent with the adsorption and desorption curve of bamboo shoot carbon in the figure. The larger specific surface area, the wider ion transport channel and better cycling performance. Therefore, the electrochemical properties of PC-1 bamboo shoot carbon were studied.

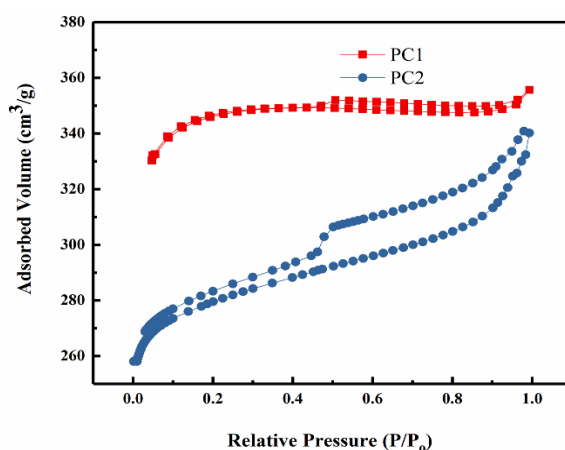


**Figure 4.** Adsorption/desorption curves of bamboo shoot carbon

The pore structure of bamboo shoot carbon can also be proved by the pore size distribution in figure 5. It can be seen from the figure that PC-1 has a large nitrogen adsorption peak at about 20 nm. It can also be seen from table 1 that the average pore size of PC-1 is 19.54 nm, which is consistent with each other. PC-2 is heat-treated at a higher temperature and the average pore diameter is also at 20 nm. It is prove that the heat treatment temperature has little effect on the size of bamboo shoots carbon, but the significant effect on the specific surface area of the hole.

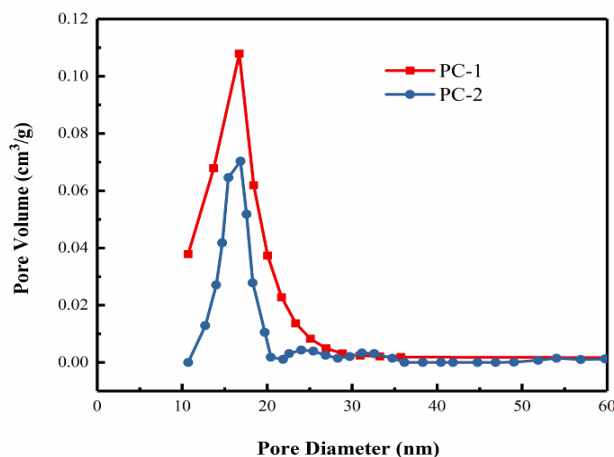


**Figure 5.** Pore size distribution of bamboo shoot carbon

Table 1 statistics the specific surface area, pore volume and pore diameter of the hole. Obviously, the specific surface area of PC-1 ( $1126.18 \text{ m}^2/\text{g}$ ) is obviously larger than PC-2 ( $657.92 \text{ m}^2/\text{g}$ ). It is should be caused by the influence of heat treatment temperature of bamboo shoot. The total pore volume and micropore volume of nitrogen adsorbed by PC-1 are  $0.55 \text{ cm}^3/\text{g}$  and  $0.50 \text{ cm}^3/\text{g}$ , respectively. The corresponding value of PC-2 drops to  $0.39 \text{ cm}^3/\text{g}$  and  $0.35 \text{ cm}^3/\text{g}$ . This result confirmed that the carbonization temperature is the main factor influencing the pore structure [14]. The higher the carbonization temperature, some micropores might collapse.

**Table 1.** Structure characteristics of bamboo shoot carbon.

CODE	$S_{\text{BET}}^{\text{a}}$ ( $\text{m}^2/\text{g}$ )	$V_{\text{total}}^{\text{b}}$ ( $\text{cm}^3/\text{g}$ )	$V_{\text{micro}}^{\text{c}}$ ( $\text{cm}^3/\text{g}$ )	Pore Size <sup>d</sup> (nm)
PC-1	1126.18	0.55	0.50	19.54
PC-2	657.92	0.39	0.35	19.37

To further understand the crystal structure of bamboo shoot carbon, XRD analysis was performed as shown in figure 6. There are two broad and weak graphitized carbon peak in the diagram, this should be the six-party lattice (002) crystal plane and (101) crystal plane shows characteristic peak according to the Bragg Equation  $2d\sin\theta=n\lambda$  can calculate the d value were  $3.64 \text{ \AA}$  and  $2.02 \text{ \AA}$ . Bamboo carbon is in the form of six-membered ring [15]. The two peaks are width and weak, which shows that a lot of free C in the carbon material.

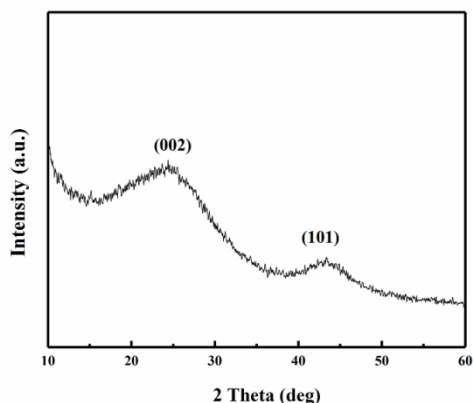


Figure 6. XRD analysis of bamboo shoot carbon.

Through XPS analysis of bamboo shoot carbon, the surface element content and chemical state of bamboo shoot carbon can be studied in figure 7. It can be seen from figure 7a that carbon, nitrogen, oxygen, phosphorus and sulfur elements exist in PC-1, and the atomic percentages are 82.5%, 2.9%, 13%, 0.6% and 1.1%, respectively. N is evenly doped into bamboo shoot carbon. The structure of N atom in bamboo shoot carbon can be determined by XPS narrow scanning as shown in figure 7b. It can be seen from the figure that a main peak at 401.1ev should be the characteristic peak of seasonal nitrogen (N-Q). Two small peaks in 399.6 ev and 398.4 ev are characteristic peaks of pyrrole nitrogen (N-5) and pyridine nitrogen (N-6) [16], confirming that N atom exists in the bamboo shoot carbon in the form of amino, imino, etc. From the above analysis, it can be concluded that the possible structure of bamboo shoot carbon is shown in figure 8.

From the above results, it can be seen that PC-1 has a large specific surface area and dense hole structure, which is suitable for use as a anode material for lithium ion batteries. Therefore, its electrochemical properties were further tested and analyzed.

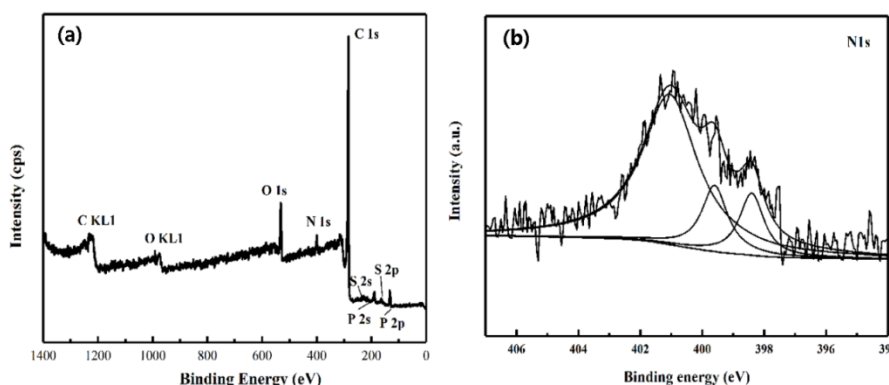
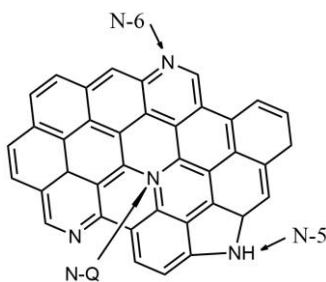
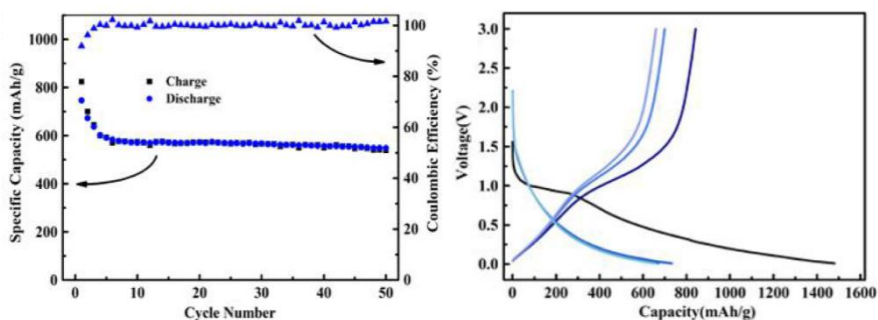


Figure 7. Survey spectra (a) and high-resolution XPS spectra (b) at N1s region of N-doped bamboo shoot carbon



**Figure 8.** Possible structure of N-doped bamboo shoot carbon



**Figure 9.** The charge-discharge data and cycling performance of PC-1

Figure 9a is the cycling performance results of PC-1 under the current density of  $0.1 \text{ A} \cdot \text{g}^{-1}$ . Figure 9b shows the first three charge and discharge curves.

As can be seen from figure 9a, the first charge and discharge of PC-1 was  $832 \text{ mAh/g}$ , and still as high as  $575 \text{ mAh/g}$  after 50 cycles, which is far higher than the petroleum carbon sold in the market. Figure 9b shows the first three charge and discharge curves of PC-1. A wide platform appears around  $1.0 \text{ v}$ . This is because the specific surface area of the material is relatively large. During the next few discharges, there was no platform in the curve because no more SEI membranes were produced [17-18]. At the same time, weak platforms can be found in the three charge-discharge curves which is the process of removing lithium ions. In addition to the lithium ions in the middle of the carbon layer, there are also many lithium ions from the nano-pore structure in the material.

The comparison of PC-1 and other anode materials were added in table 2.

**Table 2.** The specific capacity comparison of several common anode materials

Anode materials	Capacity ( $\text{mAh} \cdot \text{g}^{-1}$ , 50 cycles)	Retention rate (%, 50 cycles)
Petroleum carbon [2]	264	77.0
NiO@carbon [5]	562	84.4
Lignin carbon [8]	613	78.6
This work	575	78.2

As can be seen from table 2, traditional petroleum carbon anode materials have a lower specific capacity and the corresponding 50 cycle retention rate is also low. It is also verified that only the embedding and stripping of lithium ions exist in the charging and discharging process of petroleum carbon anode materials. The specific capacity of the battery is also proportional to the graphitization degree of the carbon material. The higher the graphitization degree, the higher the specific capacity. However, its maximum specific capacity is  $372 \text{ mAh}\cdot\text{g}^{-1}$ , which is much lower than the application of transition metal or metal oxide as anode material [19]. Ni has the highest specific capacity, which is  $1047 \text{ mAh}\cdot\text{g}^{-1}$  after 50 charge and discharge cycles, but has the defect of large expansion coefficient [20]. However, in the charging and discharging process of metallic nickel, the embedding and ejection of lithium ions tend to lead to metal embrittlement, resulting in a significant reduction in specific capacity. Lignin carbon material is also a source of biological material, but its preparation process is complicated. Compared with bamboo shoot carbon, the source and processing technology are more complex. Therefore, as a renewable carbon material, bamboo shoot have strong advantages, important scientific and application value in the field of new energy batteries.

#### 4. CONCLUSIONS

Bamboo shoot is used as the source of lithium ion carbon material, and its economic benefit is very high. It is helpful to improve the specific capacity of carbon materials by activating the pore reaming, increasing the specific surface area of carbon materials and ion transport channel. Compared with conventional petroleum carbon, the specific capacity of 50 charges and discharges is as high as  $575 \text{ mAh/g}$  and the specific capacity retention rate is 78.2%. The higher specific capacity of bamboo shoot carbon is attributed to the multistage porous structure and the doped elements such as N in the material, which increase the lattice defects of the carbon material and active sites of the reaction, resulting in higher specific capacity. Bamboo shoot carbon material can be used as the anode material of commercial battery.

#### ACKNOWLEDGEMENTS

We are thankful for the Project Supported by Zhejiang Provincial Natural Science Foundation of China Technology Project of Keqiao Innovation Research Institute of Zhejiang University of Technology (2018KQ002), (LY18E030009, LQ14E030004, LQ18E030013) and National Natural Science Foundation of China (21504079) for the support to this research.

#### References

1. X. Yin, W. Chen and J. Eom, *Energ. Policy*, 82 (2015) 233.
2. Y. Du, T. Gao and W. Ma, *Chem. Phys. Lett.*, 712 (2018) 7.
3. Q. Zhang, E. Uchaker and S.L. Candelaria, *Chem. Soc. Rev.*, 42 (2013) 3127.
4. D. Deng, M.G. Kim and J.Y. Lee, *Energ. Environ. Sci.*, 2 (2009) 818.
5. B.C. Melot and J.M. Tarascon, *Acc. Chem. Res.*, 46 (2013) 1226.
6. G. Hautier, A. Jain and S.P. Ong, *Chem. Mater.*, 23 (2011) 3495.

7. A. Jain, G. Hautier and S.P. Ong, *J. Mater. Res.*, 31 (2016) 977.
8. A. Manthiram and J. Goodenough, *J. Power Sources*, 26 (1989) 403.
9. M. Kruk, M. Jaroniec, T.W. Kim, *Chem. Mater.*, 15 (2003) 2815.
10. A.H. Lu, W. Schmidt and B. Spliethoff, *Adv. Mater.*, 15 (2003) 1602.
11. Z.P. Zhao, S.T. Shen, F. Chen, Z.P. Zhou and M.Q. Zhong, *Int. J. Electrochem. Sci.*, 14 (2019) 10058.
12. F. Chen, W.J. Zhou, H.F. Yao, P. Fan, J.T. Yang, Z.D. Fei and M.Q. Zhong, *Green Chem.*, 15 (2013) 3057.
13. K. Persson, V.A. Sethuraman and L.J. Hardwick, *J. Phys. Chem. Lett.*, 1 (2010) 1176.
14. B.P. Bastakoti, H. Oveisi and C.C. Hu, *Eur. J. Inorg. Chem.*, 7 (2013) 1109.
15. Z.P. Zhao, C.Y. Pan, G.J. Jiang and M.Q. Zhong, *Int. J. Electrochem. Sci.*, 13 (2018) 2945.
16. N. Kang, J.H. Park and J. Choi, *Angew. Chem. Int. Ed.*, 1 (2012) 6626.
17. Y. Qian, Y. Deng and X. Qiu, *Green Chem.*, 16 (2014) 2156.
18. F. Li, L. Zhang and J. Li, *J. Power. Sources.*, 292 (2015) 15.
19. G. Binotto, D. Larcher, A. Prakash, *Chem. Mater.*, 19 (2007) 3032.
20. X. Zhu, W. Wu and Z. Liu, *Electrochim. Acta*, 95 (2013) 24.

© 2020 The Authors. Published by ESG ([www.electrochemsci.org](http://www.electrochemsci.org)). This article is an open access article distributed under the terms and conditions of the Creative Commons Attribution license (<http://creativecommons.org/licenses/by/4.0/>).